# Обзор ArXiv: astro-ph, 1-14 марта 2018 года

От Сильченко О.К.

# Astro-ph: 1803.01027

## Red Misfits in the Sloan Digital Sky Survey: Properties of Star-Forming Red Galaxies

Fraser A. Evans,* Laura C. Parker, Ian D. Roberts
*Department of Physics and Astronomy, McMaster University, 1280 Main Street West, Hamilton, ON, L8S 4L8, Canada*

Accepted XXX. Received YYY; in original form ZZZ

**ABSTRACT**
We study Red Misfits, a population of red, star-forming galaxies in the local Universe. We classify galaxies based on inclination-corrected optical colours and specific star formation rates derived from the Sloan Digital Sky Survey Data Release 7. Although the majority of blue galaxies are star-forming and most red galaxies exhibit little to no ongoing star formation, a small but significant population of galaxies (~11 per cent at all stellar masses) are classified as red in colour yet actively star-forming. We explore a number of properties of these galaxies and demonstrate that Red Misfits are not simply dusty or highly-inclined blue cloud galaxies or quiescent red galaxies with poorly-constrained star formation. The proportion of Red Misfits is nearly independent of environment and this population exhibits both intermediate morphologies and an enhanced likelihood of hosting an AGN. We conclude that Red Misfits are a transition

# Выделение красных галактик с SF по данным SDSS

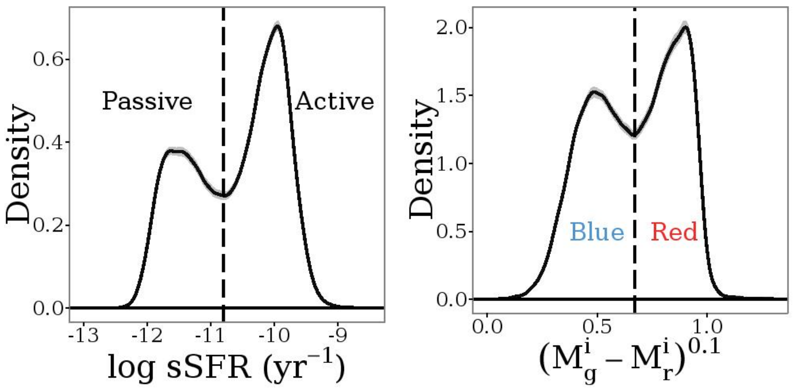


**Figure 1.** *Left*: $V_{max}$-weighted specific star formation rate (sSFR) Gaussian kernal-smoothed distribution for galaxies in the full sample. The local minimum at log(sSFR)=-10.8 $yr^{-1}$ defines our 'active' and 'passive' samples. *Right*: $V_{max}$-weighted $(M_g^i - M_r^i)^{0.1}$ colour distribution of galaxies in the full sample. A cut at $(M_g^i - M_r^i)^{0.1}$=0.67 mags defines our 'red' and 'blue' populations. Shaded regions in both plots show 99% confidence intervals from 1000 bootstrap resamplings.

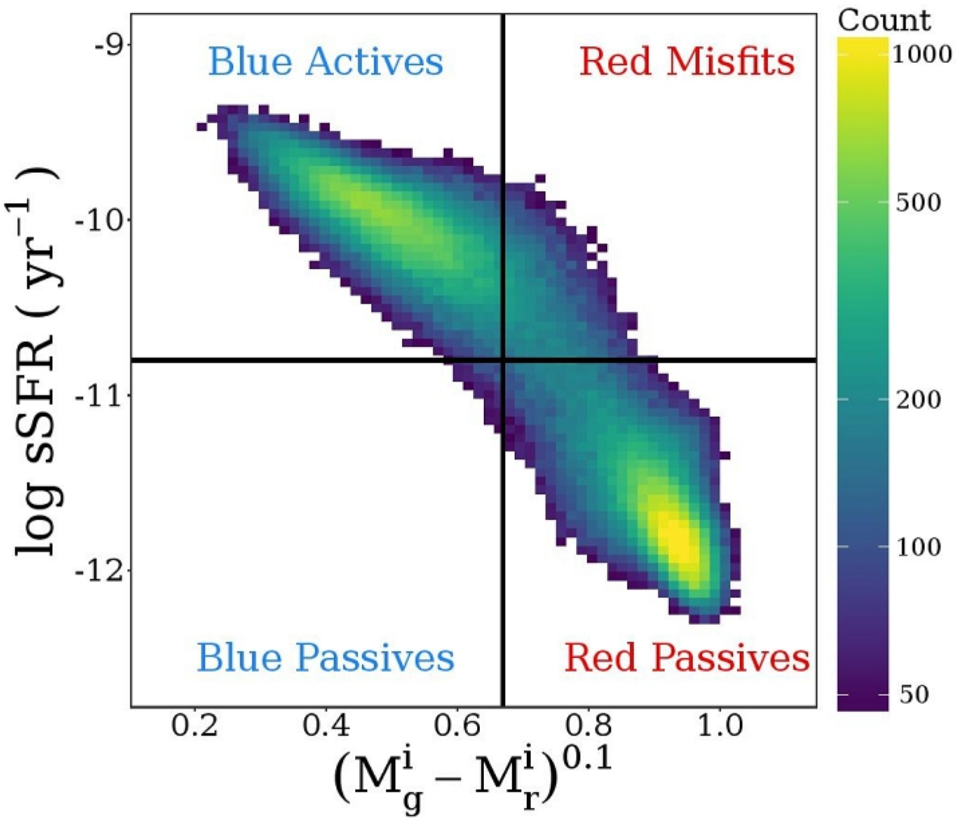

# Выборка и подвыборки

| Population | Percent of Sample | | | |
|---|---|---|---|---|
| | Full Sample (277785 galaxies) | Emission-line Sample (90000 galaxies) | Group Sample (95648 galaxies) | Isolated Sample (112614 galaxies) |
| Blue Active | 42.3% | 74.7% | 27.2% | 52.2% |
| Blue Passive | 1.7% | 1.0% | 1.6% | 1.7% |
| Red Active (Red Misfit) | 10.9% | 15.4% | 11.0% | 10.9% |
| Red Passive | 45.1% | 8.8% | 60.2% | 35.2% |

**Table 1.** Populations of each of the four galaxy populations in the four samples.

# Массы и морфология

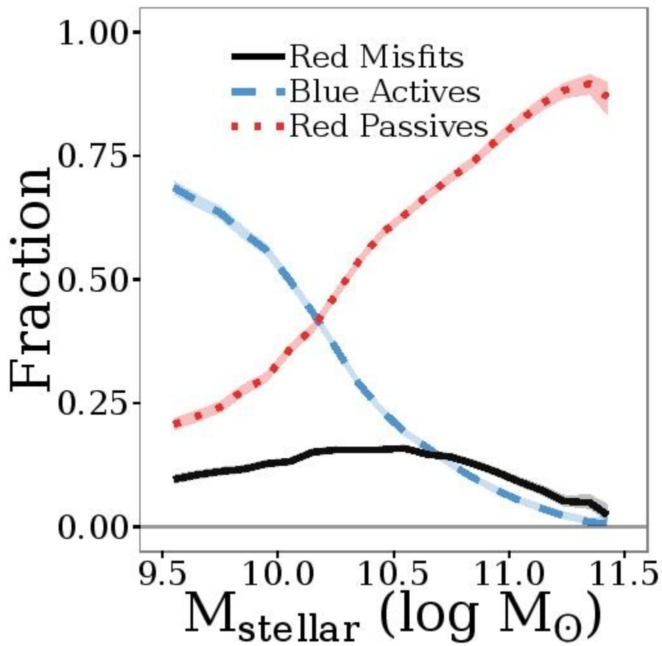


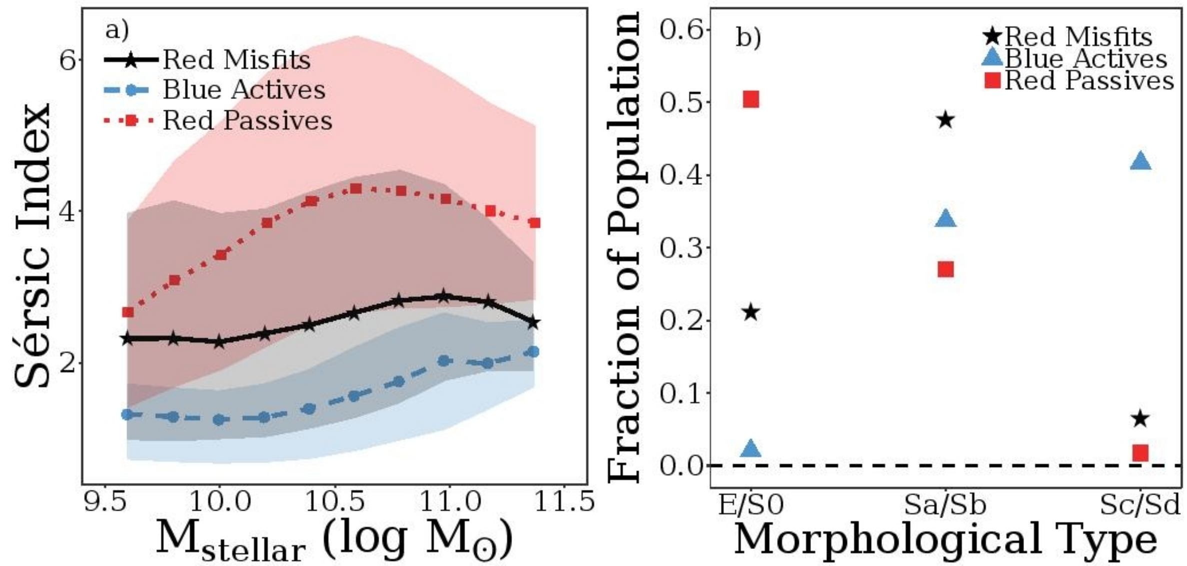


**Figure 3.** $V_{max}$-weighted relative populations of Blue Active, Red Passive and Red Misfit galaxies in the full sample binned by stellar mass. Shaded regions show 99% confidence intervals generated by

# Возбуждение и металличность

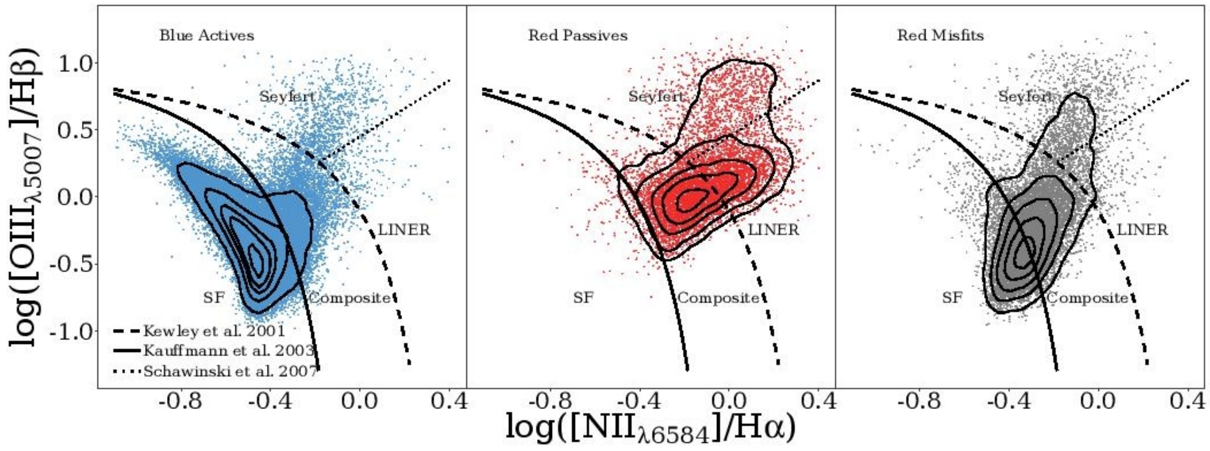


**Figure 7.** Distribution of Blue Actives (left), Red Passives (middle) and Red Misfits (right) in the emission-line sample on the BPT diagram. Contours encompass 10%, 30%, 50%, 70% and 90% of the unweighted distributions. Lines from Kewley et al. (2001) and Kauffmann et al. (2003b) define star-forming and AGN regions of the diagram as well as the composite region where emission from stellar and non-stellar processes are comparable. The dotted line from Schawinski et al. (2007) separates the AGN region into a Seyfert region and a LINER region.

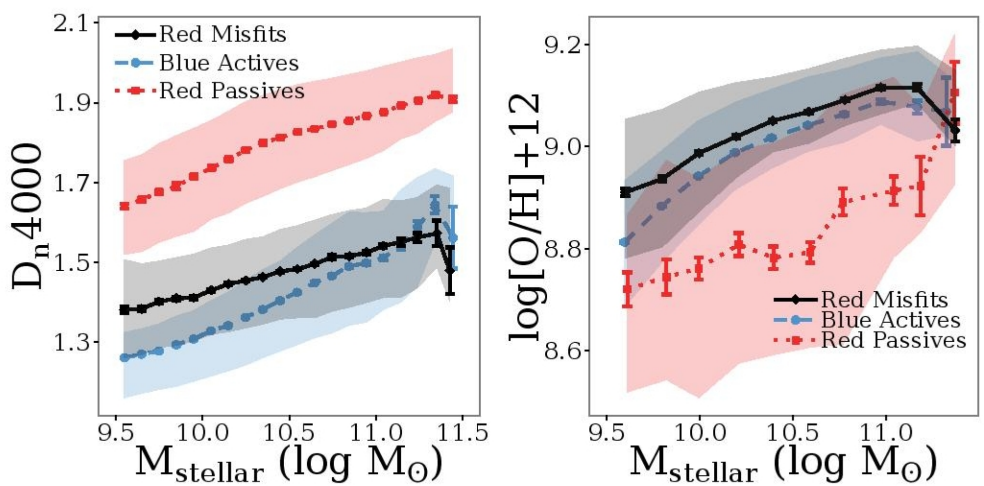


**Figure 6.** *Left:* D$_n$4000 index measurement for each population in the full sample binned by stellar mass. *Right:* Gas-phase metallicity of each population in the full sample binned by stellar mass. Error bars in both plots indicate 1$\sigma$ errors on the V$_{max}$-weighted mean value. Shaded regions span the 16th to 84th percentile of each bin.

# Плотность окружения

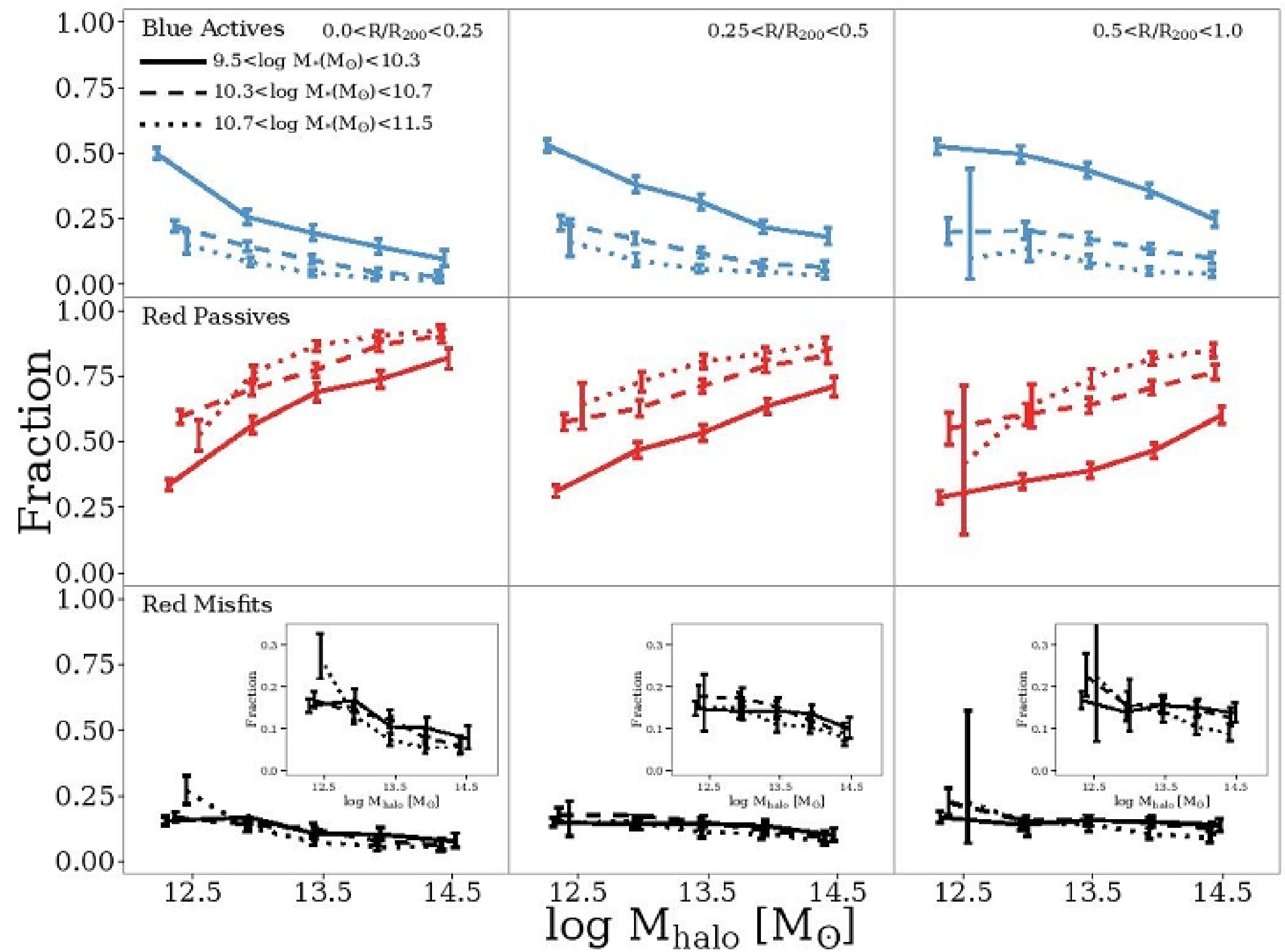


**Figure 9.** $V_{max}$-weighted satellite fractions of Blue Actives (top), Red Passives (middle) and Red Misfits (bottom) in our group sample against group halo mass. Fractions are shown for galaxies in the inner third (left column), middle third (middle column) and outer third (right column) of the $R/R_{200}$ distribution. Results are also shown in three bins of stellar mass as different line styles corresponding to the upper, middle and lower thirds of the stellar mass distribution. Insets zoom in on the Red Misfit results. Error bars are 99% confidence intervals generated by the beta distribution as outlined by Cameron (2011).

# Переходный во всех отношениях тип? Внутренний quenching?

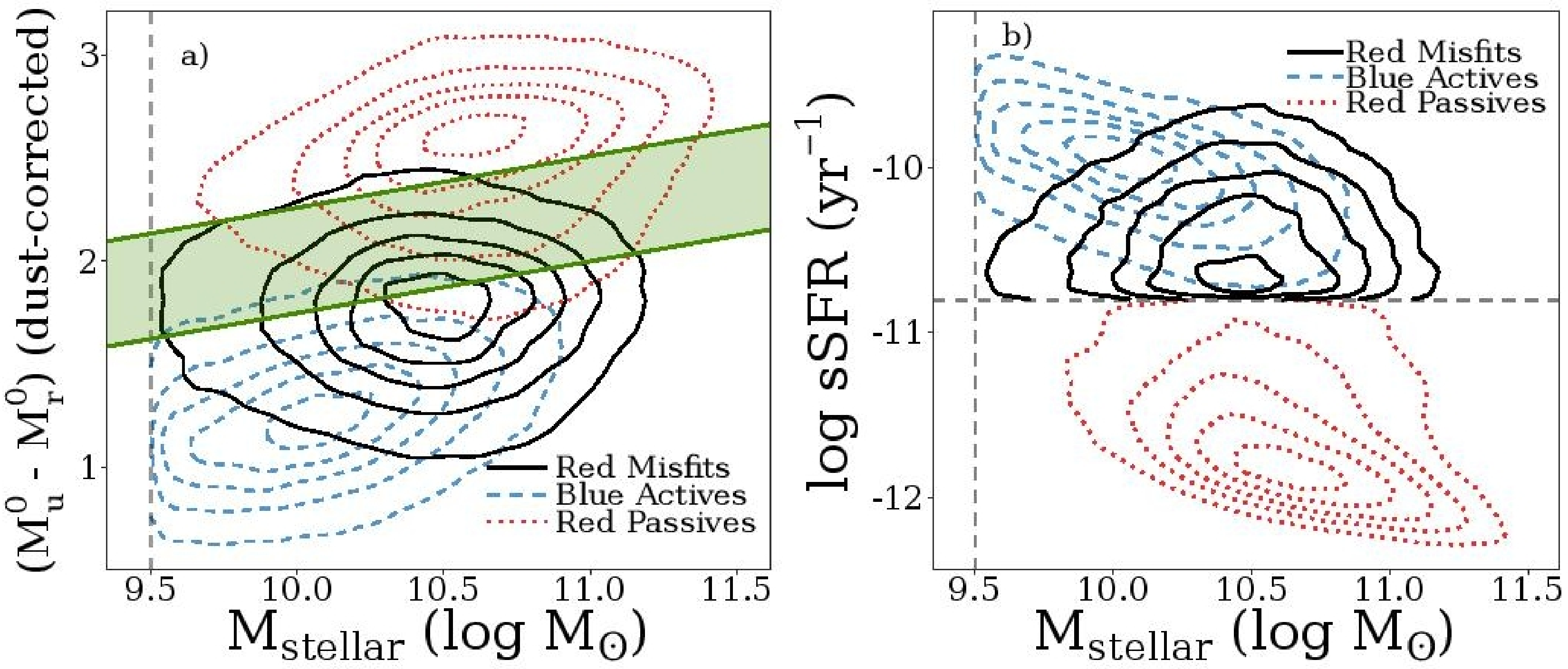


**Figure 12.** *a):* Rest-frame k-corrected $u - r$ colour against stellar mass for Red Misfits, Blue Actives and Red Passives. Colours are *not* corrected for inclination but are corrected for dust reddening using the stellar continuum $E(B-V)$ as measured by Oh et al. (2011). Shaded green region shows the green valley as defined by Schawinski et al. (2014). *b):* sSFR against stellar mass for Red Misfits, Blue Actives and Red Passives. Contours in both plots encompass 10%, 30%, 50%, 70% and 90% of the unweighted distributions. Dashed lines indicate our $M_{stellar}=10^{9.5}M_\odot$ and sSFR$=10^{-10.8}$ yr$^{-1}$ cuts.

# Astro-ph: 1803.03967

## A multi-wavelength study of the evolution of Early-Type Galaxies in Groups: the ultraviolet view

**Rampazzo R.[1], Mazzei P.[1], Marino A.[1], Bianchi L.[2], Plana, H.[3], Trinchieri G.[4], Uslenghi M.[5], Wolter A.[4]**

# Пример ультрафиолетовых колец в S0 галактике группы

**Fig. 2** *Swift*-UVOT images of NGC 1533 in the Dorado group. *Left panel*: colour composite image in the U, B, V filters (U=blue, B=green, V=red) and, *right panel*, in the W1, M2 and W2 filters (W2=blue, M2=green, W1=red). The field of view is $5' \times 5'$, North is on the top, East to the left (Rampazzo et al. 2017). Bright ring/arm-like structures are detected in ultraviolet. Furthermore, some of the ultraviolet bright regions, visible in the South-East region of the field, likely belong to NGC 1533. Indeed, the galaxy extends far beyond the optical outer ring and it is embedded in a huge HI envelope connecting it to IC 2038 (see Werk et al. 2010, and references therein)

# Остаточное (?) звездообразование в группах низкой плотности

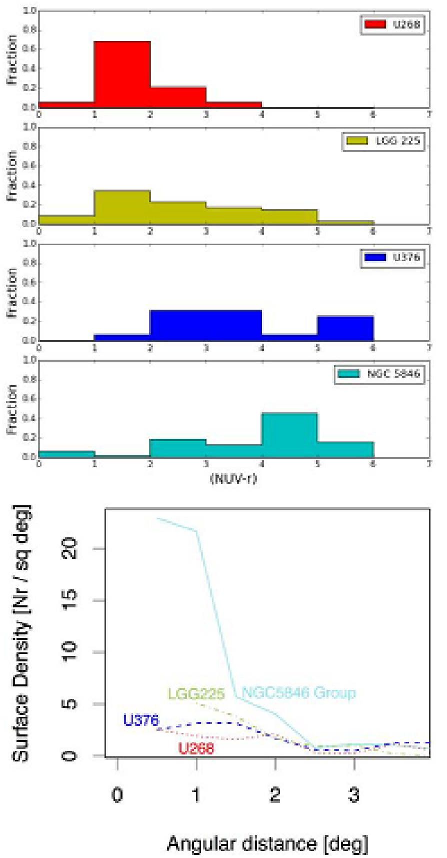


**Fig. 1** (Top panel:) The (NUV-r) colour distribution of galaxies in four groups of increasing galaxy density, namely USGC U268, LGG 225, U376 and U677 (alias NGC 5846 group). Groups have been investigated in ultraviolet by Marino et al. (2010, 2013, 2016). (Bottom panel) The surface galaxy density of the above groups as a function of the angular distance from the group centre of mass. NGC 5846 is by far the densest group with the richest Red Sequence. The surface galaxy density of U268 is slightly above the galaxy background density (adapted from Marino et al. (2016))

*Swift* offers a new perspective to study galaxies (Gehrels et al. 2004; Citterio et al. 1994; Burrows et al. 2005). It is equipped with the 30cm `UVOT` telescope with a relatively large FoV ($17' \times 17'$), $W2$ ($\lambda_0 \sim 2030$Å), $M2$ ($\lambda_0 \sim 2231$Å), $W1$ ($\lambda_0 \sim 2634$Å) ultraviolet filters and a PSF (FWHM=$2''.92$ for $W2$, $2''.45$ for $M2$, $2''.37$ for $W1$) significantly improved with respect to `GALEX`. This PSF is, in general, still to large to study the bulge of nearby galaxies. Therefore, *Swift*-`UVOT` data are useful to analyse the main body and the galaxy outskirts, which have revealed unexpected features useful to understand the evolutionary history of galaxies (Rampazzo et al. 2017).

# Вписывание закона Серсика в изображения на разных длинах волн

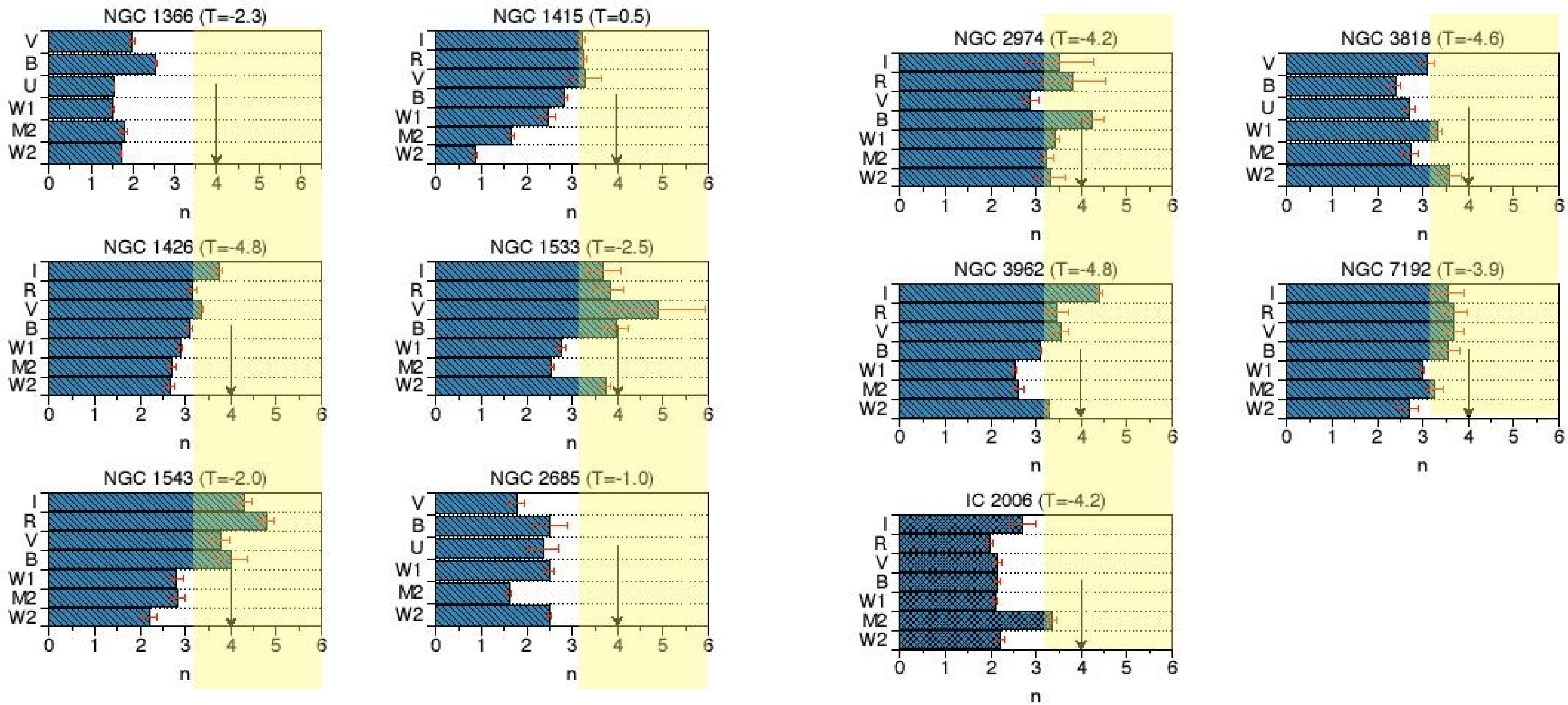


**В UV видны exp диски!**

# Astro-ph: 1803.04893

## A single population of red globular clusters around the massive compact galaxy NGC 1277

Michael A. Beasley,[1,2*] Ignacio Trujillo,[1,2] Ryan Leaman,[3] Mireia Montes,[4]

[1]Instituto de Astrofísica de Canarias, Calle Vía Láctea, La Laguna, Tenerife, Spain

[2]University of La Laguna. Avda. Astrofísico Fco. Sánchez, La Laguna, Tenerife, Spain

[3]Max-Planck Institut für Astronomie, Königstuhl 17, D-69117, Heidelberg, Germany

[4]Department of Astronomy, Yale University, 06511 New Haven, CT, USA

**Massive galaxies are thought to form in two phases: an initial, early collapse of gas and giant burst of central star formation, followed by the later accretion of material that builds up their stellar and dark matter haloes (*1*) (*2*) (*3*) (*4*). The globular cluster systems of such galaxies are believed to form in a similar manner. The initial central burst forms metal-rich (red) clusters, while more metal-poor (blue) clusters are brought in by the later accretion of less massive satellites (*5*) (*6*) (*7*) (*8*) (*9*) (*10*). This formation process is thought to lead**

# Компактная галактика раннего типа

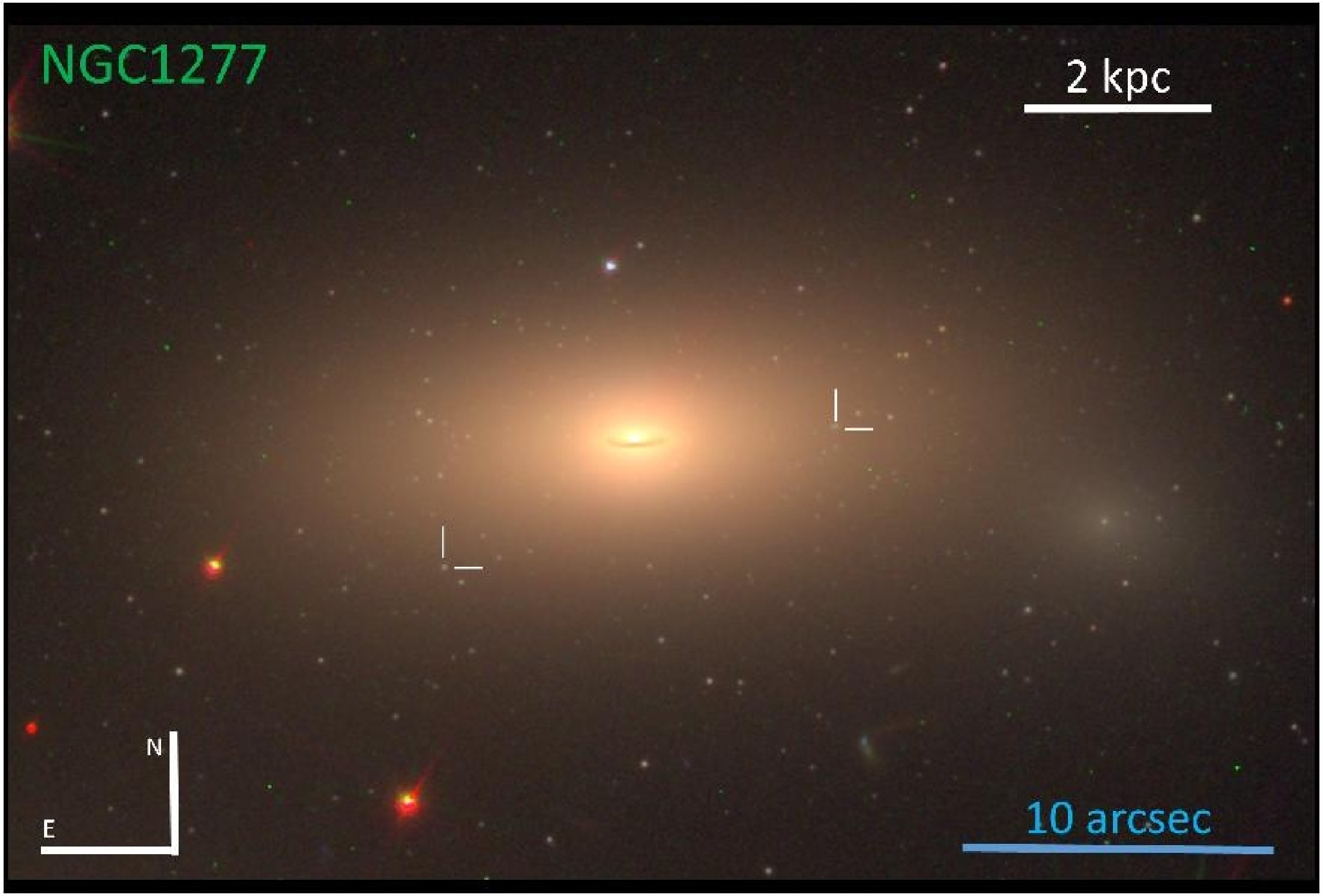


**Extended data Fig. 1. Colour composite ($g_{475W}$, $r_{625W}$, $z_{850LP}$) HST image of the massive relic galaxy NGC 1277.** The $g_{475W}$ and $z_{850LP}$ imaging was obtained with the HST

# Плотность распределения шаровых скоплений

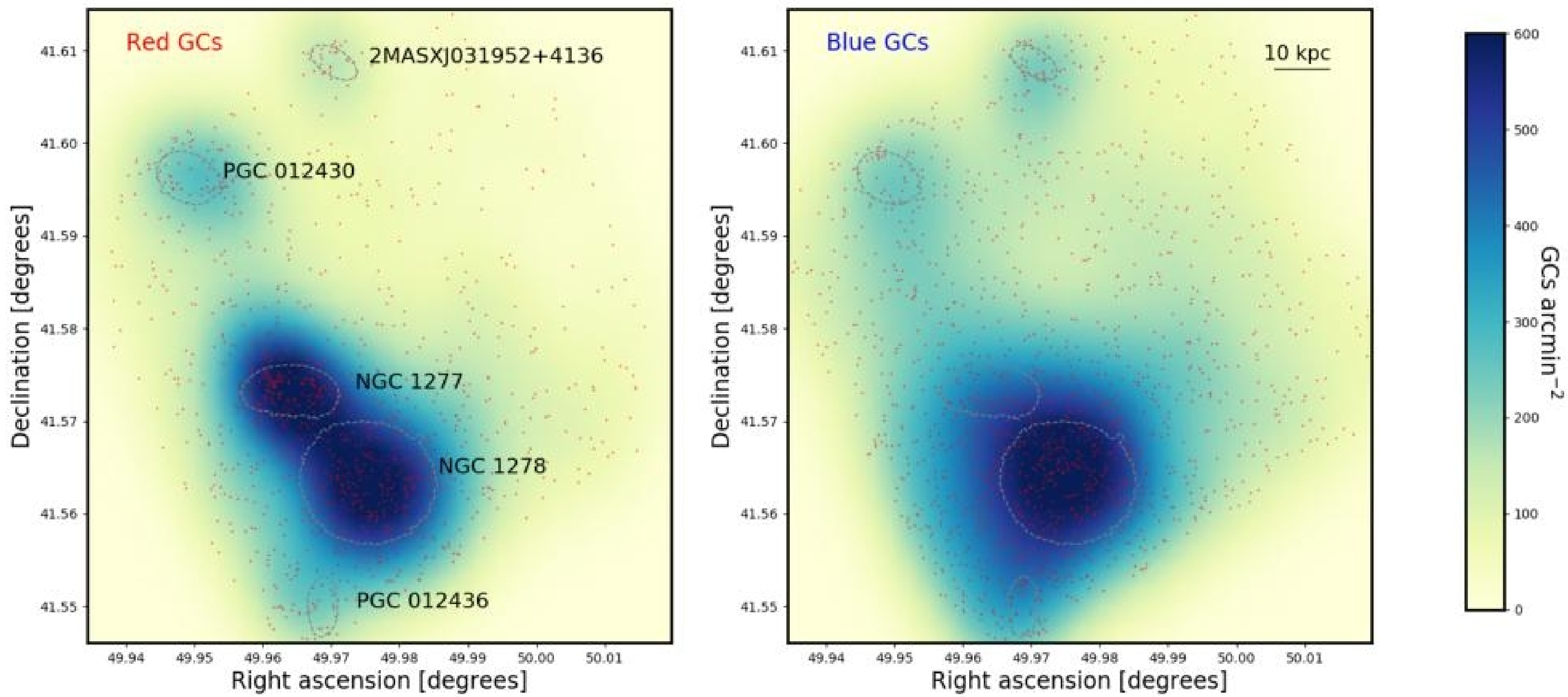


**Fig. 1. Spatial distribution of clusters in HST/ACS field.** North is up, East is to the right here. Individual clusters are shown as points. The locations of galaxies are indicated by galaxy isophotes corresponding to 23 mag arcsec$^{-2}$ in $g_{475W}$. NGC 1277 is to left of centre in the plots, with the neighbouring galaxy NGC 1278 located some 50 arcseconds ($\sim$ 17 kpc) to the South East in projection. The red and blue clusters have been separated by taking a cut at $(g_{475W} - z_{850LP})_0 = 1.15$, typical of the peak separation between the red and blue clusters in galaxies of this stellar mass (*11*). Overplotted is a gaussian kernel density estimate map

# Унимодальное распределение цвета шаровых скоплений NGC 1277

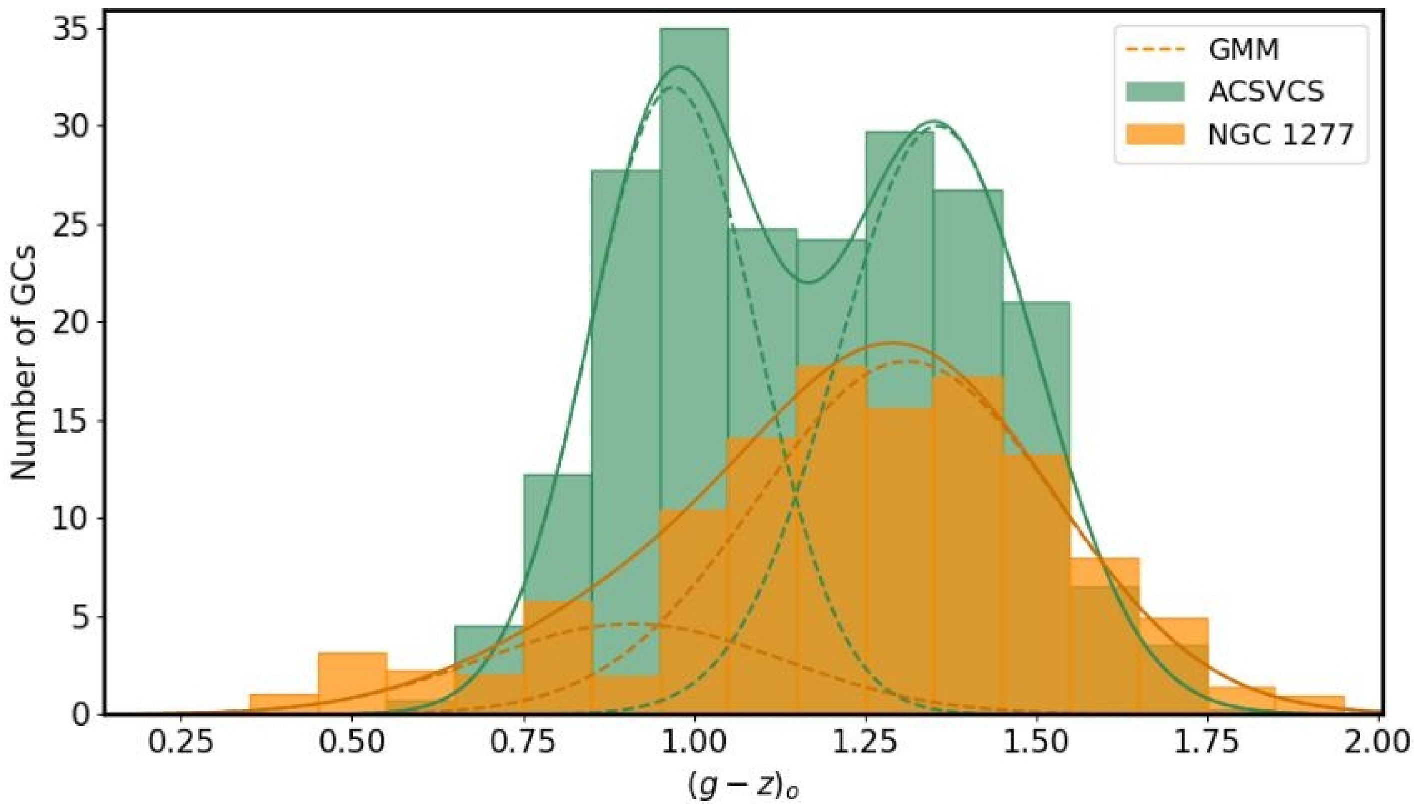


**Fig. 2. The colour distribution of clusters in NGC 1277 compared to composite cluster system.** The colour distribution for NGC 1277 has been constructed for the entire radial extent of its cluster system (to 11 kpc), and has been corrected for the contamination from NGC 1278 clusters which, in projection, is 17 kpc from NGC 1277. The composite cluster system was constructed from four galaxies from (*11*) with similar stellar masses to NGC 1277 ($M_* \sim 1.2 \times 10^{11} M_\odot$). The dashed curves indicated Gaussian components of the cluster systems obtained

# Заниженная доля голубых скоплений для данной массы галактики

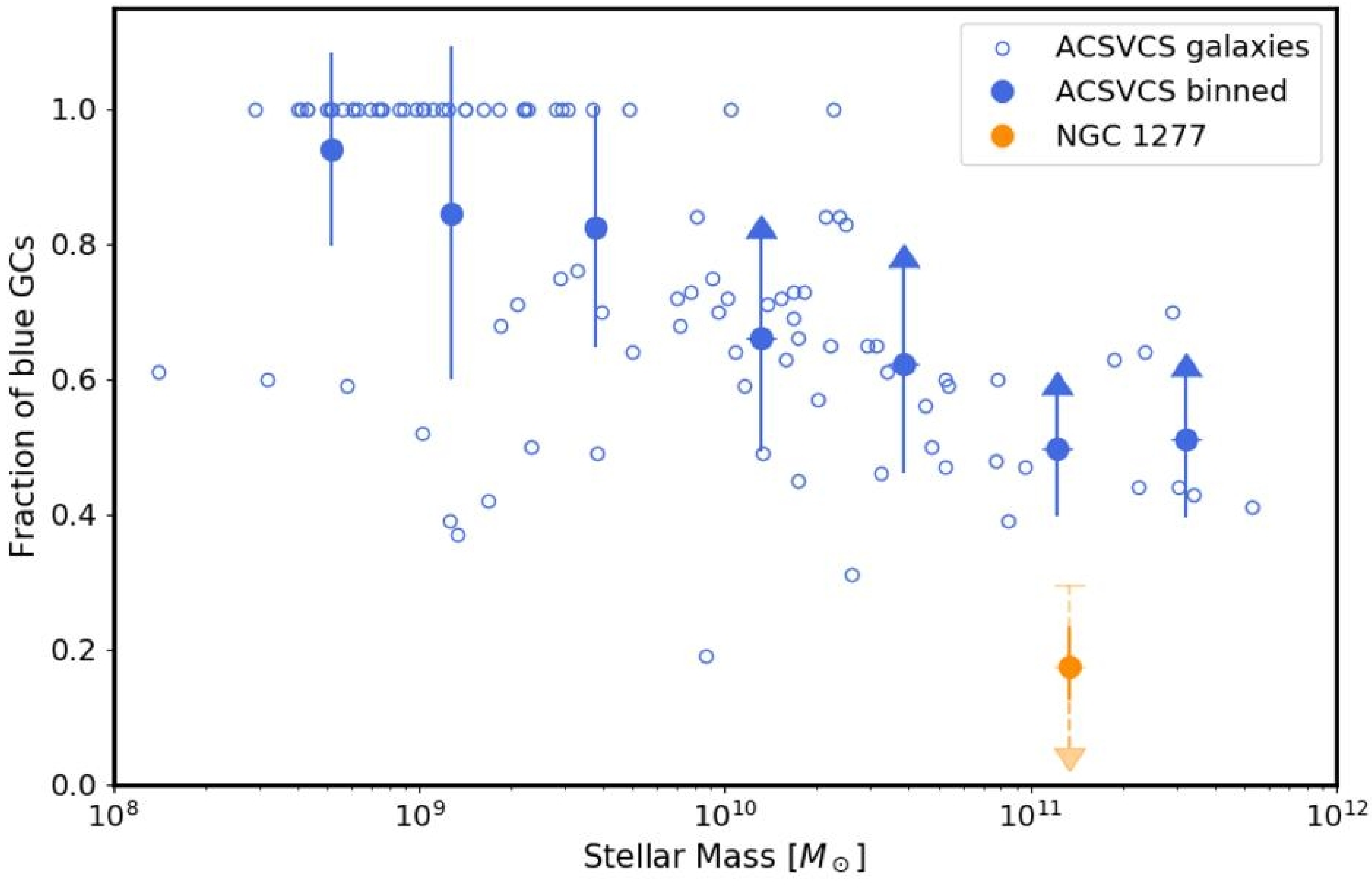


;. **3. The fraction of blue clusters in galaxies of a given stellar mass.** Data for the
vey galaxies comes from (11). The figure shows that NGC 1277 has a very small (or zero)

# Astro-ph: 1803.04770

## Spatial Distribution of Globular Clusters in the Galaxy

N. R. Arakelyan,[1,2]* S. V. Pilipenko,[2] N. I. Libeskind[3]
[1] *Moscow Institute of Physics and Technology, Dolgoprudny, Institutskiy per., 9, Moscow Region, 141701, Russia*
[2] *P.N. Lebedev Physical Institute of Russian Academy of Sciences, 84/32 Profsojuznaja Street, 117997 Moscow, Russia*
[3] *Leibniz–Institut für Astrophysik, Potsdam, An der Sternwarte 16, D–14482 Potsdam, Germany*

Accepted XXX. Received YYY; in original form ZZZ

**ABSTRACT**
The Milky Way's satellite galaxies and Globular Clusters (GCs) are known to exhibit an anisotropic spatial distribution. We examine in detail this anisotropy by the means of the inertia tensor. We estimate the statistical significance of the results by repeating this analysis for random catalogues which use the radial distribution of the real sample. Our method reproduces the well-known planar structure in the distribution of the satellite galaxies. We show that for GCs several anisotropic structures are observed. The GCs at small distances, $2 < R < 10$ kpc, show a structure coplanar with the Galactic plane. At smaller and larger distances the whole sample of GCs shows quite weak anisotropy. Nevertheless, at largest distances the orientation of the structure is close to that of the satellite galaxies, i.e. perpendicular to the Galactic plane. We estimate the probability of random realization for this structure of 1.7%. The Bulge-Disk GCs show a clear disk-like structure lying within the galactic disk. The Old Halo GCs show two structures: a well pronounced polar elongated structure at $R < 3$ kpc which is perpendicular to the galactic plane, and a less pronounced disk-like structure

# Посчитали тензоры инерции – для систем спутников и шаровых скоплений

use two different tensors: the inertia tensor and the reduced tensor, which are constructed as follows:

$$S_{ij} = \frac{1}{N}\sum_{k=1}^{N} x_i^k x_j^k, \quad (1)$$

$$J_{ij} = \frac{1}{N}\sum_{k=1}^{N} \frac{x_i^k x_j^k}{R_k^2}, \quad (2)$$

where $S$ is the inertia tensor, $J$ is the reduced tensor, $N$ is the number of objects, $x_i^k$ is the distance from $k$-th object to the center of the Galaxy along $i$-th coordinate axis, $R_k^2 = x_k^2 + y_k^2 + z_k^2$, $R$ is the distance to each $k$-th particle. The three eigenvalues of the inertia tensor (a,b and c) are sorted in increasing order such that a>b>c. The degree of the anisotropy is characterized by the ratios of the eigenvalues, $c/a$ and $b/a$, both of which approach to 1 in case of isotropic distribution. The eigenvectors of the tensor give us the directions of anisotropy.

# Просто проекция распределений

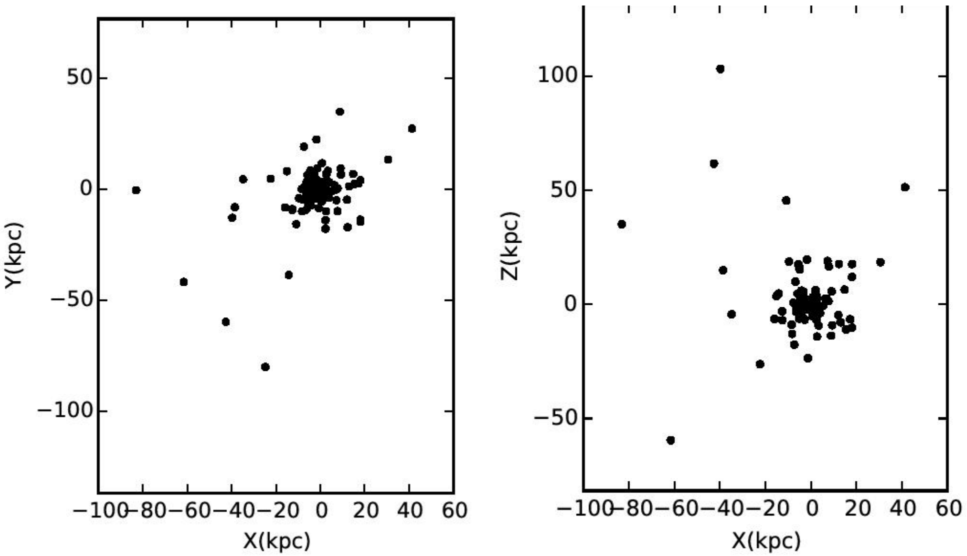


**шаровые скопления**

**спутники**

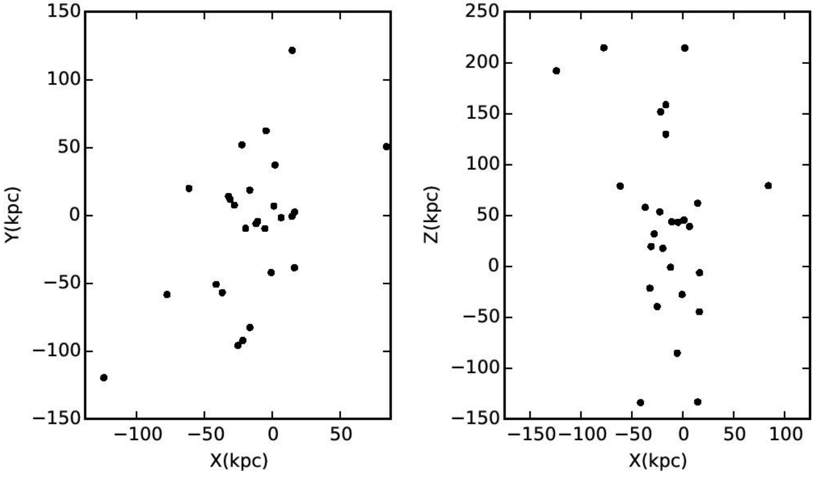

# Тензоры инерции

**шаровые скопления**

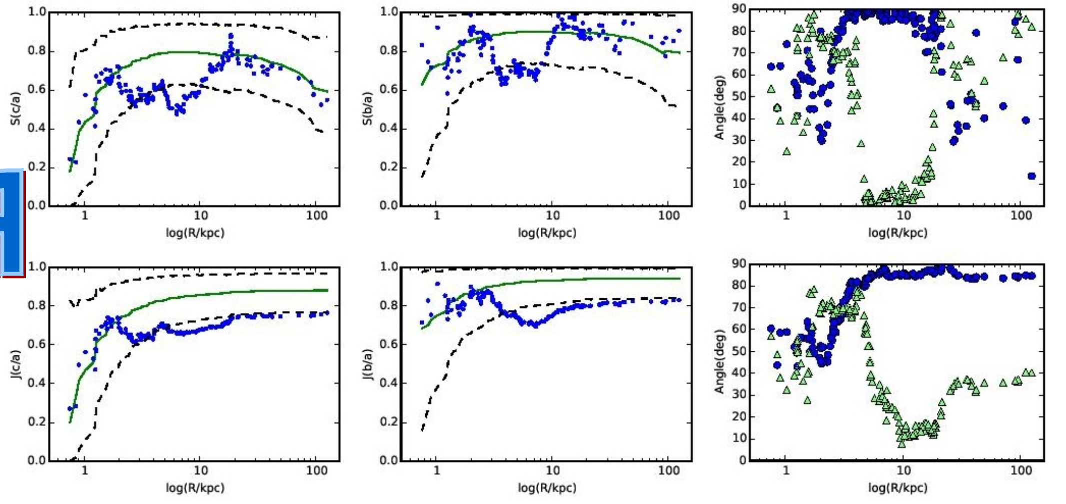


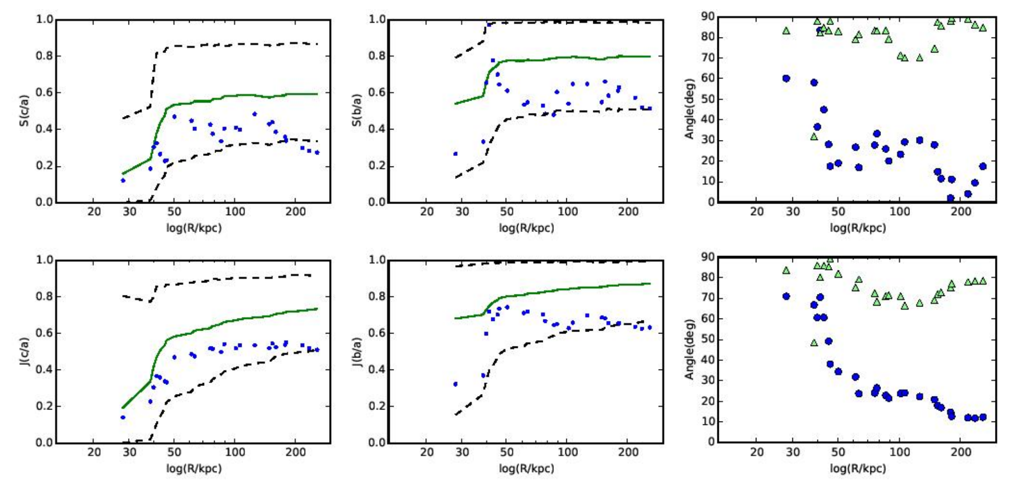


**Figure 5.** The Anisotropy of 27 satellite galaxies quantified by the inertia tensor (equation (1), top row) and the reduced inertia tensor (equation (2), bottom row). The left column shows the distribution of $c/a$ as function of satellite galactocentric distance. The middle column shows the distribution of $b/a$ as a function of galactocentric distance. Each blue dot represents the cumulative eigenvalue ratio of these tensors computed for all galaxies *interior* to that position. The solid green line represents the median eigenvalue ratios for 10,000 random samples that maintain the same radial distribution as the data, but whose polar and azimuthal angle has been randomised. The dashed lines represent the $\pm 3\sigma$ of such random distributions. The right column shows the angle, measured in degrees, subtended between the Milky Way′s galactic pole and the major (blue dots) and the minor (green triangles) axis of the two inertia tensors. Green triangles close to 90 deg indicate a polar plane.

**спутники**

# Разбиение шаровых скоплений на подсистемы диска и гало

Скопления диска – в диске на R>3 кпк

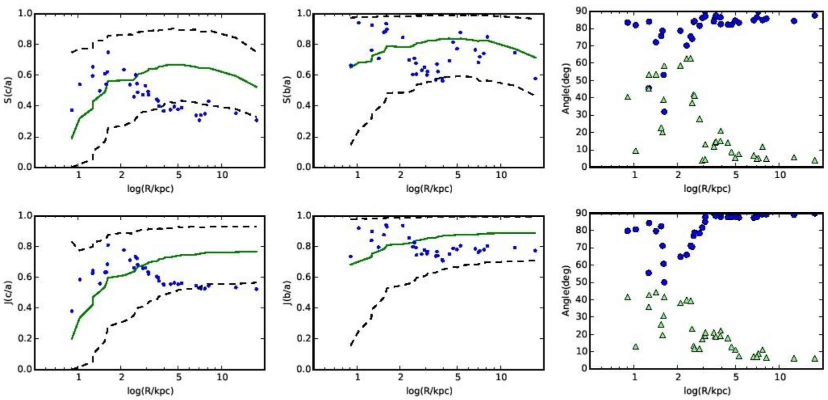


Старые скопления гало изотропны

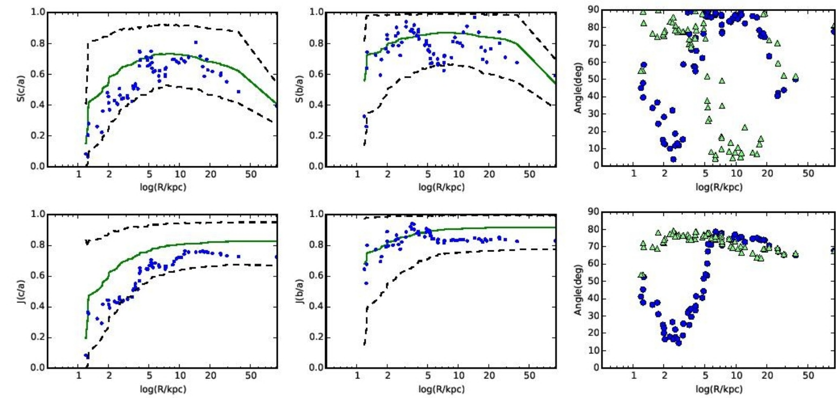


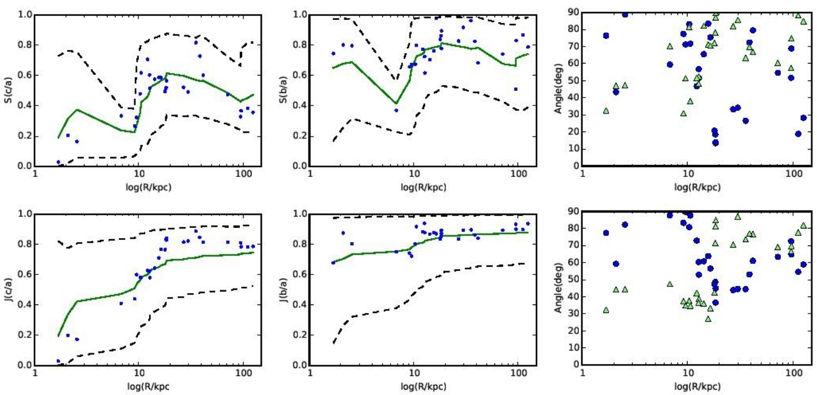


«молодые» скопления гало НЕ анизотропно распределены

**Table 3.** Direction of axes for different samples

| Sample | Major axis l | Major axis b | Minor axis l | Minor axis b |
|---|---|---|---|---|
| All GCs | 71° | 76° | 126° | −8° |
| GCs ($2 < R < 10$) | −4° | 2° | −103° | 80° |
| All SGs [1] | −132° | 73° | 154° | −5° |
| 11 SGs [1] | −143° | 64° | 153° | −12° |
| All BD | −32° | −3° | 21° | 86° |
| BD ($R > 3$) | −33° | −3° | 20° | 85° |
| All OH | 3° | −12° | 91° | 9° |
| OH ($R < 3$) | −104° | 78° | 99° | 11° |
| OH ($6 < R < 20$) | −148° | −16° | 122° | 1° |
| All YH | 62° | 62° | 142° | −5° |

1) SGs – satellite galaxies.